

Passive Magnetic Shielding in Gradient Fields

C.P. Bidinosti^{1, a)} and J.W. Martin¹

Physics Department, The University of Winnipeg, 515 Portage Avenue, Winnipeg, MB, R3B 2E9, Canada.

(Dated: 31 October 2013)

The effect of passive magnetic shielding on dc magnetic field gradients imposed by both external and internal sources is studied. It is found that for concentric cylindrical or spherical shells of high permeability material, higher order multipoles in the magnetic field are shielded progressively better, by a factor related to the order of the multipole. In regard to the design of internal coil systems for the generation of uniform internal fields, we show how one can take advantage of the coupling of the coils to the innermost magnetic shield to further optimize the uniformity of the field. These results demonstrate quantitatively a phenomenon that was previously well-known qualitatively: that the resultant magnetic field within a passively magnetically shielded region can be much more uniform than the applied magnetic field itself. Furthermore we provide formulae relevant to active magnetic compensation systems which attempt to stabilize the interior fields by sensing and cancelling the exterior fields close to the outermost magnetic shielding layer. Overall this work provides a comprehensive framework needed to analyze and optimize dc magnetic shields, serving as a theoretical and conceptual design guide as well as a starting point and benchmark for finite-element analysis.

PACS numbers: 41.20.Gz,24.80.+y,21.10.Ky

I. INTRODUCTION

Passive magnetic shielding systems typically use a concentric arrangement of thin shells of a high permeability material to divert magnetic field lines around a region of interest. The region within the shielding system consequently possesses a reduced local magnetic field.

While magnetic shielding is useful for a variety of applications, the most stringent requirements are found in high precision experiments where the limits of magnetometry technology are experienced or are themselves being studied. Some recent examples are in biomagnetism^{1,2}, electric dipole moment experiments^{3,4}, and in developments of the most precise atomic magnetometers⁵⁻⁷.

Neutron electric dipole moment (EDM) experiments in particular suffer from a systematic effect relating to the accrual of geometric phase as neutrons and comagnetometer atoms sample the experimental volume⁸⁻¹¹. The geometric phase effect is expected to present a dominant systematic effect in future neutron EDM experiments. To first approximation, the systematic correction is proportional to the first-order gradient along the direction of the applied magnetic field $\partial B_z / \partial z$. It is therefore important in these experiments both to limit and to characterize magnetic field gradients.

While the analysis and development of single- and multi-layer magnetic shields has been an important and active area of research for well over a century¹²⁻²⁵, the focus in analytical treatments has been almost exclusively on shielding uniform magnetic fields. To the best

of our knowledge, only Urankar and Oppelt²³ have explored the issue of passive magnetic shielding in gradient fields from an analytical perspective.

Sumner *et al.*²¹ provide an excellent overview of the history of the field of magnetic shielding. Exact solutions for concentric cylindrical and spherical shields^{12,13,15} have been simplified to approximate formulae valid in the limit of high magnetic permeability and thin shells^{14,16-21} as well as to provide axial shielding factors for cylindrical geometries. More recently, axial shielding in relation to shield spacing, end cap holes, and gaps between mating surfaces has been explored numerically^{24,25}. Analytic treatments of the quasi-static solutions have led to developments in external active compensation²².

However, as mentioned above, these authors considered only uniform applied fields. Urankar and Oppelt²³ analyzed the general multipole field (both as an external and internal source) for single spherical shields, and provided general shielding and reaction factors. They employed their results to analyze active magnetic compensation used in conjunction with magnetically shielded rooms. Quasi-static solutions valid in the dc limit were provided. We extend this work (in the dc limit) to multi-layer shields with spherical as well as infinite cylindrical geometry. For each, we consider the following situations:

1. *Externally applied fields.* Calculations are included both single and multi-layer shields. The shielding factor for general multipole fields is calculated internal to the innermost shield and is of principal interest. The field external to the outermost shield is also calculated, and is useful for designing active magnetic compensation systems. This field is dominated by the response of the outermost layer and the analysis is restricted to a single shield only.

2. *Internally applied fields.* In many cases, such as in EDM experiments, a highly homogeneous inter-

^{a)}Author to whom correspondence should be addressed. Electronic mail:c.bidinosti@uwinnipeg.ca

nal field is desired and this is generally supplied by a coil system internal to a set of magnetic shields. We consider here the impact of the innermost magnetic shield on general internally produced multipole fields, and calculate reaction factors by which the field internal to the coil system is amplified.

We comment here on our primary new results:

- We report shielding factors, interior reaction factors, and exterior response fields for single layer, infinite cylindrical magnetic shields, exposed to general multipole dc applied fields. This extends the work of Ref.²³ from spherical to cylindrical geometries; for the spherical case, we demonstrate agreement with Ref.²³. Our results for single-layer shields are useful for designing active magnetic compensation systems (in the case of exterior response fields) and internal coil systems (in the case of interior reaction factors), and we provide useful examples of this.
- We provide shielding factors for multi-layer shields in both cylindrical and spherical geometries for general multipole fields. One of our primary results is that higher multipole fields are always shielded better than the homogeneous field, a general result that should prove useful in applications requiring homogeneous fields. This extends previous work to general multipole fields, and extends the work of Ref.²³ to multi-layer shielding systems in the dc limit.
- Finally, we use a somewhat unique method of solution compared to previous authors, in that we consider the equivalent problem of bound surface currents. While the end results are of course equivalent, our approach may be useful in certain situations. We found, for example, that the consideration of surface currents gives a more direct conceptual link to the coils and current structures that one ultimately uses.

Our work is valid for dc fields, general multipole sources (both internal and external to the magnetic shield), and any number of concentric shields (cylindrical or spherical). We provide an exact treatment valid for shields of any permeability μ and thickness. We also provide new approximate formulae in the high- μ , thin shell limit, which we have now validated for all higher multipoles.

We proceed first by describing our general method and then the cylindrical and spherical applications of the method. We conclude with applications to some geometries of interest in EDM experiments, which as noted above have very stringent requirements for magnetic field quality.

II. PROBLEM STATEMENT AND METHOD OF SOLUTION USING EQUIVALENT BOUND SURFACE CURRENTS

Two problems of particular geometry are solved here using standard cylindrical and spherical coordinates: (i) the interaction of the transverse, 2-dimensional magnetic field $\mathbf{B} = B_\rho(\rho, \phi)\hat{\rho} + B_\phi(\rho, \phi)\hat{\phi}$ with infinitely-long cylindrical shells, and (ii) the interaction of the general magnetic field $\mathbf{B} = B_\rho(\rho, \theta, \phi)\hat{\rho} + B_\theta(\rho, \theta, \phi)\hat{\theta} + B_\phi(\rho, \theta, \phi)\hat{\phi}$ with spherical shells.

As is commonly done to achieve analytic solutions for passive shielding problems, we restrict our analysis to shields of linear, homogeneous media, carrying no free current. Under such conditions, the response of a permeable object to an applied magnetic field can be recast solely in terms of bound surface current \mathbf{K}_b on the surfaces of the object. As a result, we take advantage of known formulae for the magnetic fields of cylindrical and spherical sheet currents^{26–28} to solve the appropriate boundary conditions for sets of concentric magnetic shields.

For a shielding system of M concentric shells, there are $2M$ distinct surface currents contributing to the net magnetic field in each region. Satisfying the boundary condition

$$\begin{aligned} H_{\text{in}}^{\parallel} &= H_{\text{out}}^{\parallel} \\ \text{or} \\ \frac{1}{\mu_{\text{in}}} B_{\text{in}}^{\parallel} &= \frac{1}{\mu_{\text{out}}} B_{\text{out}}^{\parallel} \end{aligned} \quad (1)$$

for the tangential component of the magnetic field results in a set of $2M$ simultaneous equations that determine the magnitudes of the unknown surface currents. By contrast, the typical means of solution using the magnetic scalar potential (see e.g. Ref.²⁹) gives a set of $4M$ simultaneous equations, albeit resulting in a sparser matrix.

III. THE INFINITELY LONG CYLINDRICAL SHIELD

A. The 2D multipole field generated by a cylindrical current sheet

From Refs.^{26–28}, an axial surface current

$$\mathbf{K} = K \sin(n\phi) \hat{z} \quad (2)$$

with n -fold rotational symmetry ($n \geq 1$) bound to a cylindrical surface $\rho = a$ gives rise to the vector potential

$$\mathbf{A} = \mathcal{K} \frac{\sin(n\phi)}{n} \begin{cases} \rho^n \hat{z} & \rho < a \\ \frac{a^{2n}}{\rho^n} \hat{z} & \rho > a \end{cases}, \quad (3)$$

where $\mathcal{K} = \mu_0 K / (2a^{n-1})$ has units T/m^{n-1} . The introduction of \mathcal{K} , while not necessary, leads to a simplified

notation for the determination of shielding factors, especially when multiple shields are considered. The magnetic field arising from Eq. 3 is

$$\mathbf{B} = \mathcal{K} \begin{cases} \rho^{n-1} [\cos(n\phi) \hat{\mathbf{p}} - \sin(n\phi) \hat{\mathbf{\phi}}] & \rho < a \\ \frac{a^{2n}}{\rho^{n+1}} [\cos(n\phi) \hat{\mathbf{p}} + \sin(n\phi) \hat{\mathbf{\phi}}] & \rho > a \end{cases}. \quad (4)$$

We use these results to solve the following problems.

B. A single cylindrical shield in an external field

Consider an infinitely-long cylindrical shield of inner radius R , thickness t , and permeability μ in the presence of an externally applied transverse magnetic field

$$\mathbf{B}_{\text{ext}} = G_n \rho^{n-1} [\cos(n\phi) \hat{\mathbf{p}} - \sin(n\phi) \hat{\mathbf{\phi}}] \quad (5)$$

with a magnitude gradient G_n in T/mⁿ⁻¹. The case $n = 1$ therefore corresponds to a uniform field, and $n > 1$ corresponds to higher multipoles. By symmetry, the bound currents induced on the inner surface ($r_1 = R$) and outer surface ($r_2 = R + t$) of the magnetic shield have the same harmonic n as B_{ext} and generate fields given by Eq. 4.

To find the coefficients \mathcal{K}_1 and \mathcal{K}_2 , representative of the bound surface current on the inner and outer surfaces of the shield, respectively, the boundary condition of Eq. 1 is applied to the azimuthal components B_ϕ of the magnetic field. This results in the following system of equations:

$$(\mu + \mu_0) \mathcal{K}_1 + (\mu - \mu_0) \mathcal{K}_2 = -(\mu - \mu_0) G_n \quad (6)$$

$$(\mu - \mu_0) \left(\frac{r_1}{r_2} \right)^{2n} \mathcal{K}_1 + (\mu + \mu_0) \mathcal{K}_2 = (\mu - \mu_0) G_n, \quad (7)$$

which have solutions

$$\mathcal{K}_1 = -2G_n \frac{\mu(\mu - \mu_0)}{(\mu + \mu_0)^2 - (r_1/r_2)^{2n} (\mu - \mu_0)^2} \quad (8)$$

and

$$\mathcal{K}_2 = G_n \frac{\mu^2 - \mu_0^2 + (r_1/r_2)^{2n} (\mu - \mu_0)^2}{(\mu + \mu_0)^2 - (r_1/r_2)^{2n} (\mu - \mu_0)^2}. \quad (9)$$

Defining the shielding factor S as the applied field divided by the net internal field^{16,17,20,21} gives

$$\begin{aligned} S &= \frac{G_n}{\mathcal{K}_1 + \mathcal{K}_2 + G_n} \\ &= \frac{(\mu + \mu_0)^2 - (r_1/r_2)^{2n} (\mu - \mu_0)^2}{4\mu\mu_0} \end{aligned} \quad (10)$$

$$= 1 + \frac{(\mu - \mu_0)^2}{4\mu\mu_0} \left[1 - \left(\frac{r_1}{r_2} \right)^{2n} \right]. \quad (11)$$

In the limit $R \gg t$ and $\mu \gg \mu_0$, this reduces to

$$S \simeq 1 + \frac{\mu}{\mu_0} \frac{n}{2} \frac{t}{R}, \quad (12)$$

where $\bar{R} = R + t/2$ is the average radius of the shield.

The results of Eqs. 11 and 12 for the $n = 1$ case (i.e., a uniform applied field) agree with previous work.^{12,16,17,20–22,30–32} The important new result here is the generalization to higher n , where we find that higher multipoles are always shielded better than $n = 1$ case. In the thin shield limit, in particular, the shielding factor increases proportional to n . Taking a linear combination of external fields, summing Eq. 5 over n , we would therefore find that the interior shielded volume always becomes more uniform, i.e. the higher multipoles are suppressed more strongly.

We now consider the *exterior* field $\mathbf{B}_{\text{shield}}$, defined as the additional field induced by the presence of the magnetic shield. An important consideration for active shielding systems (which feed back on measurements of the net magnetic field outside the passive shield assembly) is the perturbation $\mathbf{B}_{\text{shield}}$ superimposed on the applied field in the region $\rho > r_2$. From Eqs. 4, 8 and 9, the general solution is

$$\mathbf{B}_{\text{shield}} = \frac{\mathcal{K}_1 r_1^{2n} + \mathcal{K}_2 r_2^{2n}}{\rho^{n+1}} [\cos(n\phi) \hat{\mathbf{p}} + \sin(n\phi) \hat{\mathbf{\phi}}], \quad (13)$$

which for $\mu \gg \mu_0$ reduces to

$$\mathbf{B}_{\text{shield}} = G_n \frac{r_2^{2n}}{\rho^{n+1}} [\cos(n\phi) \hat{\mathbf{p}} + \sin(n\phi) \hat{\mathbf{\phi}}]. \quad (14)$$

This in turn can be recast as

$$\mathbf{B}_{\text{shield}} = \frac{\mu_0}{4\pi} \frac{m'_n}{\rho^{n+1}} [\cos(n\phi) \hat{\mathbf{p}} + \sin(n\phi) \hat{\mathbf{\phi}}], \quad (15)$$

where $m'_n = 4\pi G_n r_2^{2n} / \mu_0$ is the $(n+1)^{\text{th}}$ multipole moment per unit length defined by

$$\mathbf{A} = \frac{\mu_0 m'_n \sin(n\phi)}{4\pi} \frac{\hat{\mathbf{z}}}{n \rho^n} \quad (16)$$

for the vector potential outside a current-carrying cylinder from Eq. 3.

The result for the exterior field is important because it may also be applied to multi-layer shielding systems, since it is the response of the outermost shield that dominates. Furthermore, as in the magnetic shielding case above, the exterior field may be decomposed into multipoles. The results can therefore be used to decide the optimal placement of the magnetic sensors in the active magnetic compensation system, because the sensors can be placed selectively to accentuate sensitivity to particular multipoles, considering also the steeper suppression of higher multipoles with increasing ρ .

C. Multiple shields in an external field

Now consider a set of M concentric cylinders in an applied external field given by Eq. 5. The geometry is shown in Fig. 1, where our conventions for labelling are also described. The m -th cylinder has an inner radius R_m , an outer radius $R_m + t_m$, a thickness t_m and a permeability μ_m . There are now $2M$ bound surface currents that one must find. The i -th surface current \mathcal{K}_i resides on the *inner* surface of the m -th shield if i is odd (i.e., $i = 2m - 1$) and on its *outer* surface if i is even (i.e., $i = 2m$). The radial position of \mathcal{K}_i is thus defined as

$$r_i = \begin{cases} R_m & \text{for } i = \text{odd and } m = \frac{i+1}{2} \\ R_m + t_m & \text{for } i = \text{even and } m = \frac{i}{2}, \end{cases} \quad (17)$$

i.e. $r_1 = R_1$ is the inner surface of the innermost shield, $r_2 = R_1 + t_1$ is the outer surface of the innermost shield, $r_3 = R_2$ is the inner surface of the next-to-innermost shield, and so on.

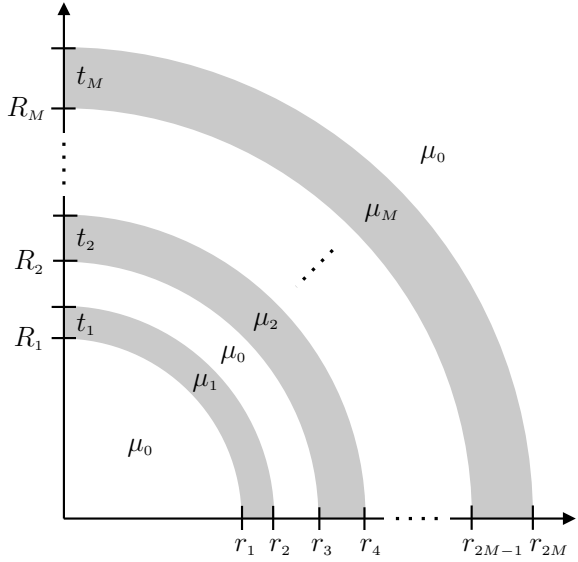


FIG. 1. Cross-sectional view (first quadrant) of M concentric cylindrical or spherical shells separated by free space. The material boundaries are located at radial positions r_1 through r_{2M} . The inner radius R , thickness t , and permeability μ of each shield is indicated on the drawing.

Satisfying the boundary condition of Eq. 1 at each surface leads to the general system of equations

$$\mathbf{A}\mathbf{K} = G_n \mathbf{I}, \quad (18)$$

where $\mathbf{I} = [1, 1, \dots, 1]^T$, $\mathbf{K} = [\mathcal{K}_1, \mathcal{K}_2, \dots, \mathcal{K}_{2M}]^T$, and \mathbf{A} is a $2M \times 2M$ matrix with elements

$$a_{ij} = \begin{cases} (r_j/r_i)^{2n} & \text{for } j < i \\ U_m & \text{for } j = i = \text{odd and } m = \frac{i+1}{2} \\ V_m & \text{for } j = i = \text{even and } m = \frac{i}{2} \\ -1 & \text{for } j > i \end{cases}, \quad (19)$$

where

$$U_m = -V_m = -\frac{\mu_m + \mu_0}{\mu_m - \mu_0}, \quad (20)$$

and r_i and r_j are defined per Eq. 17. The 2×2 diagonal submatrices of \mathbf{A} correspond to Eqs. 6 and 7 for each individual, isolated shield. To illustrate, the explicit form of the general matrix \mathbf{A} for $M = 2$ shields is

$$\mathbf{A} = \begin{pmatrix} -\frac{\mu_1 + \mu_0}{\mu_1 - \mu_0} & -1 & -1 & -1 \\ \left(\frac{R_1}{R_1 + t_1}\right)^{2n} & \frac{\mu_1 + \mu_0}{\mu_1 - \mu_0} & -1 & -1 \\ \left(\frac{R_1}{R_2}\right)^{2n} & \left(\frac{R_1 + t_1}{R_2}\right)^{2n} & -\frac{\mu_2 + \mu_0}{\mu_2 - \mu_0} & -1 \\ \left(\frac{R_1}{R_2 + t_2}\right)^{2n} & \left(\frac{R_1 + t_1}{R_2 + t_2}\right)^{2n} & \left(\frac{R_2}{R_2 + t_2}\right)^{2n} & \frac{\mu_2 + \mu_0}{\mu_2 - \mu_0} \end{pmatrix}.$$

Returning now to the general case, the total combined shielding factor for M concentric cylindrical shields is

$$S_{\text{tot}} = G_n \left(G_n + \sum_{i=1}^{2M} \mathcal{K}_i \right)^{-1}, \quad (21)$$

with the \mathcal{K}_i determined from Eqs. 18 and 19. An algebraic scheme for the solution of Eq. 21 is given by Wills¹², and one can show that our result agrees with his explicit formulation of S_{tot} for double and triple cylindrical shields of the same permeability μ . With the generating formulae of Eq. 19, Eq. 18 is also readily coded and solved using any number of computer programs designed for symbolic or numeric computation.³³

The results of solving these equations for multi-layer shields, along with approximate formulae valid for the small- t , high- μ limit, will be discussed in Section V. A key generic feature will be the suppression of higher n in powers of the number of shields.

D. A single cylindrical shield with an internal coil

We now turn to the study of coil systems internal to the magnetic shield system. In this case, the modification of the internal field is dominated by the innermost magnetic shield. We therefore consider a single cylindrical shield in order to simplify the discussion.

Consider an applied surface current \mathbf{K} of the form Eq. 2 on a coaxial cylindrical surface $\rho = a$ inside a single shield of inner radius $r_1 = R$, outer radius $r_2 = R + t$, and permeability μ . Solving boundary conditions gives the following system of equations:

$$(\mu - \mu_0) \left(\frac{a}{r_1} \right)^{2n} \mathcal{K}_a - (\mu + \mu_0) \mathcal{K}_1 - (\mu - \mu_0) \mathcal{K}_2 = 0 \quad (22)$$

$$(\mu - \mu_0) \left(\frac{a}{r_2} \right)^{2n} \mathcal{K}_a + (\mu - \mu_0) \left(\frac{r_1}{r_2} \right)^{2n} \mathcal{K}_1 + (\mu + \mu_0) \mathcal{K}_2 = 0, \quad (23)$$

where $\mathcal{K}_a = \mu_0 K / (2a^{n-1})$. The equations are again solved for \mathcal{K}_1 and \mathcal{K}_2 .

The ratio of field in the region $r < a$, divided by the field without the shield may then be calculated. We call this ratio the reaction factor C , in keeping with the terminology of Ref.²³. The result for the reaction factor is

$$C = \frac{\mathcal{K}_a + \mathcal{K}_1 + \mathcal{K}_2}{\mathcal{K}_a} \quad (24)$$

$$= 1 + \left(\frac{a}{r_1} \right)^{2n} \frac{(\mu - \mu_0)(\mu + \mu_0)\gamma_n}{4\mu\mu_0 + (\mu - \mu_0)^2\gamma_n} \quad (25)$$

where $\gamma_n \equiv 1 - (r_1/r_2)^{2n}$. In the limit $\mu \gg \mu_0$ this reduces to

$$C = 1 + \left(\frac{a}{R} \right)^{2n}, \quad (26)$$

and one sees that the internal field is augmented more strongly for small n than it is for large n because $a < R$. In the limit $a = R$, the reaction factor is identically 2, independent of n .

These results are applied to a sample internal coil design in Sec. V. A key feature will again be that fields are in general more homogeneous with the shield than without, but that optimal homogeneity can be achieved for a particular geometrical factor a/R .

IV. THE SPHERICAL SHIELD

A. The zonal multipole field generated by a spherical current sheet

In general, a surface current bound to a sphere, and its resulting magnetic field, can be written in terms of spherical harmonics of order m and degree n ^{26,27}. One can show, however, that the resulting equations arising from the boundary conditions on the tangential components of the magnetic field (i.e., B_θ and B_ϕ) are independent of the order m of the spherical harmonic. Without loss of generality, we can therefore restrict the analysis of spherical shields to zonal surface currents and fields only (i.e., ϕ -independent, $m = 0$), a simplification also noted by Urankar and Oppelt²³.

The results for a given n can therefore be applied, without loss of generality, to cases where tesseral components (i.e., $m > 0$) exist in the fields and currents. This is extremely valuable from the point of view of coil design, where the general spherical harmonics can be used as *building blocks* to produce a desired magnetic field³⁴.

From Refs.^{26,27}, the zonal surface current

$$\mathbf{K} = K P_n^1(u) \hat{\phi} \quad (27)$$

bound to a spherical surface $r = a$ gives rise to the vector potential

$$\mathbf{A} = \mathcal{K} P_n^1(u) \begin{cases} r^n \hat{\phi} & r < a \\ \frac{a^{2n+1}}{r^{n+1}} \hat{\phi} & r > a \end{cases}, \quad (28)$$

where $P_n^1(u)$ is the associated Legendre function of order 1 and degree n , $u = \cos\theta$, and the coefficient $\mathcal{K} = \mu_0 K / ((2n+1)a^{n-1})$ has units T/mⁿ⁻¹. The magnetic field arising from Eq. 28 is

$$\mathbf{B} = \mathcal{K} \begin{cases} r^{n-1} (n+1) [nP_n(u) \hat{\mathbf{r}} - P_n^1(u) \hat{\theta}] & r < a \\ \frac{a^{2n+1}}{r^{n+2}} n [(n+1)P_n(u) \hat{\mathbf{r}} + P_n^1(u) \hat{\theta}] & r > a \end{cases}, \quad (29)$$

where $P_n(u)$ is the Legendre function of degree n . We use these results to solve the following problems.

B. A single spherical shield in an external field

Consider a spherical shield of inner radius $r_1 = R$, outer radius $r_2 = R + t$, and permeability μ in the presence of an externally applied magnetic field

$$\mathbf{B}_{\text{ext}} = G_n r^{n-1} [n(n+1)P_n(u) \hat{\mathbf{r}} - (n+1)P_n^1(u) \hat{\theta}] \quad (30)$$

with a magnitude gradient G_n in T/mⁿ⁻¹. The method of analysis follows exactly as above, and the solution of the boundary conditions on the tangential field B_θ leads to the general shielding factor

$$S = 1 + \frac{(\mu - \mu_0)^2}{\mu\mu_0} \frac{n(n+1)}{(2n+1)^2} \left[1 - \left(\frac{r_1}{r_2} \right)^{2n+1} \right], \quad (31)$$

which agrees with Ref.²³. In the limit of a thin shield ($t \ll R$) with large permeability ($\mu \gg \mu_0$), the shielding factor can be approximated as

$$S \simeq 1 + \frac{\mu}{\mu_0} \frac{n(n+1)}{2n+1} \frac{t}{R}. \quad (32)$$

The results of Eqs. 31 and 32 for the $n = 1$ case (i.e., a uniform applied field) agree with previous authors^{12,15,29}. Similar to the cylindrical case, higher n fields are shielded progressively better, and in the large- n limit the shielding factor again becomes proportional to n . In cases where the applied magnetic field would be a linear combination of fields with differing n , the magnetic field internal to the magnetic shield would therefore always be more uniform than the applied field, i.e., higher multipoles are suppressed more strongly.

We now again consider the *exterior* field induced by the presence of the magnetic shield in the region $r > r_2$. In this case, the perturbation of the external field by a spherical shield of $\mu \gg \mu_0$ is

$$\begin{aligned} \mathbf{B}_{\text{shield}} &= G_n (n+1) \frac{r_2^{2n+1}}{r^{n+2}} [(n+1)P_n(u) \hat{\mathbf{r}} + P_n^1(u) \hat{\theta}] \\ &= \frac{\mu_0}{4\pi} \frac{m_n}{r^{n+2}} [n(n+1)P_n(u) \hat{\mathbf{r}} + nP_n^1(u) \hat{\theta}], \end{aligned} \quad (33)$$

where $m_n = 4\pi G_n r_2^{2n+1} (n+1)/(n\mu_0)$ is the $(n+1)^{\text{th}}$ multipole moment defined by

$$\mathbf{A} = \frac{\mu_0 m_n}{4\pi r^{n+1}} P_n^1(u) \hat{\phi} \quad (34)$$

for the vector potential outside a current-carrying sphere from Eq. 28.

C. Multiple spherical shields in an external field

For M concentric shields, we again have the same system of equations $\mathbf{A}\mathbf{K} = G_n \mathbf{I}$ where now the general matrix elements of \mathbf{A} are

$$a_{ij} = \begin{cases} \frac{n}{n+1} (r_j/r_i)^{2n+1} & \text{for } j < i \\ U_m & \text{for } j = i = \text{odd and } m = \frac{i+1}{2} \\ V_m & \text{for } j = i = \text{even and } m = \frac{i}{2} \\ -1 & \text{for } j > i \end{cases}, \quad (35)$$

with

$$U_m = -\frac{(n+1)\mu_m + n\mu_0}{(n+1)(\mu_m - \mu_0)}, \quad (36)$$

$$V_m = \frac{n\mu_m + (n+1)\mu_0}{(n+1)(\mu_m - \mu_0)}, \quad (37)$$

and r_i and r_j are defined per Eq. 17. In general the total combined shielding factor for M concentric spherical shields is given by Eq. 21 with the \mathcal{K}_i determined from Eqs. 18 and 35.

One can show that the general shielding factor of Eq. 21 reduces to the explicit formula for double and triple spherical shields of the same permeability.^{12,15}

We calculate sample results for multi-layer magnetic shields in Section V. Similar to the cylindrical case, a generic feature will be a suppression of higher $n > 1$ and a more uniform resultant internal shielded field.

D. A single spherical shield with an internal coil

Again driven by the desire to create an internal coil system that is homogeneous, we consider internal coils wound on a spherical surface inside the magnetic shielding system. As in the cylindrical case, the modification of the internal field will be dominated by the response of the innermost magnetic shield, and we restrict the analysis to a single spherical shield.

Consider an applied surface current \mathbf{K} of the form Eq. 27 on $r = a$ inside a spherical shield of inner radius $r_1 = R$, outer radius $r_2 = R + t$, and permeability μ . Following the method laid out in Sec. III D, the reaction factor giving the ratio of field in the region $r < a$ with

and without the shield is

$$C = 1 + \left(\frac{a}{r_1}\right)^{2n+1} \times \frac{n(\mu - \mu_0)(n(\mu + \mu_0) + \mu_0)\gamma_n}{(2n+1)^2\mu\mu_0 + n(n+1)(\mu - \mu_0)^2\gamma_n}, \quad (38)$$

where now $\gamma_n = 1 - (r_1/r_2)^{2n+1}$. In the limit $\mu \gg \mu_0$ this reduces to

$$C = 1 + \frac{n}{n+1} \left(\frac{a}{R}\right)^{2n+1}. \quad (39)$$

These results agree with Ref.²³. An interesting difference with the cylindrical case is the prefactor $n/(n+1)$ preceding the second term. Because of it, there is a cross-over behaviour in the relative magnitudes of the reaction factors and one finds that higher order fields become augmented more strongly (not less) by the presence of the shield as $a/R \rightarrow 1$. This is discussed further in Sec. V C.

V. RESULTS AND APPLICATIONS

A. Multiple shields: Numerical results and useful approximations

Most practical interests lie in the construction of multiple shields made of thin material ($t_m \ll R_m$) with large permeability ($\mu_m \gg \mu_0$). Many previous authors provided approximations for designing shields in this regime. A well-known result, for the total shielding factor S_{tot} for well-separated shields^{16,18,21}, is generalized to any n as follows:

$$S_{\text{tot}} \simeq \prod_{m=1}^{M-1} S_M S_m \left[1 - \left(\frac{\bar{R}_m}{\bar{R}_{m+1}} \right)^\beta \right], \quad (40)$$

where S_m is the shielding factor of the m -th shield (from Eq. 12 or 32), \bar{R}_m is the average radius of the m -th shield, and the exponent β equals $2n$ for cylinders and $2n+1$ for spheres.

In Figs. 2 and 3 we compare Eq. 40 with the general result of Eq. 21 for cylindrical and spherical shields, respectively. We analyze a shield geometry that is likely typical of many applications: four concentric shields each of the same thickness $t = \frac{1}{16}$ inches ~ 1.6 mm (a standard size) with a radius $R_1 = 0.5$ m for the inner most shield. All shields have the same permeability and we examine two specific cases: $\mu = 2 \times 10^4 \mu_0$ and $\mu = 4 \times 10^4 \mu_0$. The shield spacings are set by a single geometrical scale factor k , such that the inner radius of the m -th shield is $R_m = (1+k)^{m-1} R_1$.

A key feature is that higher n are always progressively suppressed as n increases. For example, for the four-layer shield explored here, the shielding factor for $n = 2$ is of order 10^2 greater than for $n = 1$. The optimal choice of scale factor k is relatively independent n .

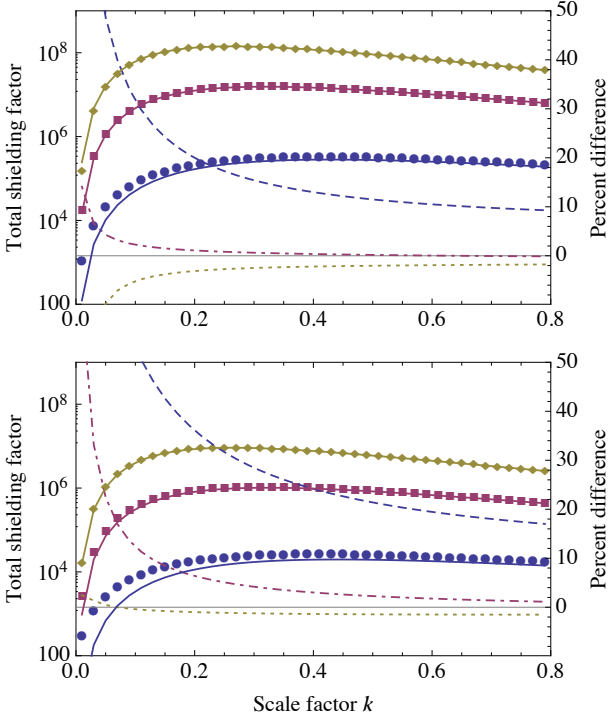


FIG. 2. The total shielding factor of four concentric cylindrical shells of permeability $\mu/\mu_0 = 4 \times 10^4$ (top) and 2×10^4 (bottom) determined from Eq. 21 for an applied field of $n = 1$ (blue circles), 2 (red squares), and 3 (yellow diamonds). The solid lines are the results of Eq. 40. The right ordinate axis gives the percent difference between Eqs. 21 and 40 for $n = 1$ (dashed line), 2 (dot-dashed line), and 3 (dotted line).

Furthermore, the approximate formulae of Eq. 40 appear to be even more accurate for higher n than for the $n = 1$ case. This is shown in Figs. 2 and 3 as a percent difference from the exact result.

For closely packed cylindrical and spherical shields, on the other hand, a useful approximation for the total shielding factor is

$$S_{\text{tot}} \simeq \sum_{m=1}^M S_m, \quad (41)$$

which is now validated for all n . For shields that just touch, Eq. 41 correctly approximates the shielding factor of a single shield with thickness equivalent to the total thickness of the shielding material. As an example, we show in Fig. 4 plots of S_{tot} as a function of a small separation d between each of the four concentric cylindrical shields discussed above. Similar results hold for spherical shields.

At $d = 0$, we find that for the range of parameters studied here Eq. 41, using Eq. 12 for the S_m , over predicts S_{tot} by $\sim 3 - 5\%$ compared to the exact result of Eq. 21. This is reduced slightly if one uses Eq. 11 for the S_m . We also point out, that as expected, the value of S_{tot} from Eq. 21 for the four shields with $d = 0$ agrees exactly with Eq. 11 for a single shield that is four times as thick.

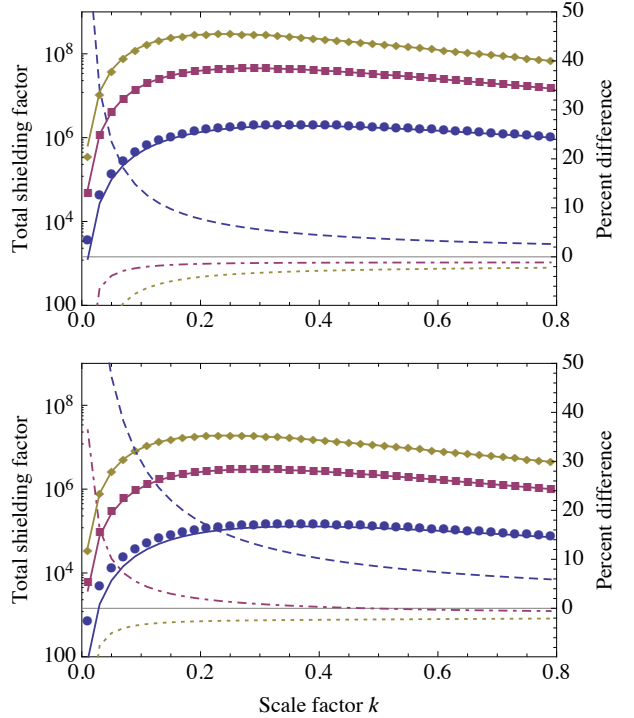


FIG. 3. The total shielding factor of four concentric spherical shells of permeability $\mu/\mu_0 = 4 \times 10^4$ (top) and 2×10^4 (bottom) determined from Eq. 21 for an applied field of $n = 1$ (blue circles), 2 (red squares), and 3 (yellow diamonds). The solid lines are the results of Eq. 40. The right ordinate axis gives the percent difference between Eqs. 21 and 40 for $n = 1$ (dashed line), 2 (dot-dashed line), and 3 (dotted line).

The results of Fig. 4 also highlight the importance of sufficiently separating the shells. An interesting observation is that the shielding of higher order $n > 1$ fields increases dramatically with n with even sub-millimetre shield spacing. This may argue for subdividing shields further, possibly with thin interstitial nonmagnetic layers, if desiring particularly to reduce gradients with relatively less impact on the uniform field case. For example, an application requiring better control of $n > 1$ could use four well-separated shields to reduce $n = 1$, but each of those four shields could be thinner layers separated by a thin plastic layer to relatively augment the shielding of $n > 1$.

B. The external physical dipole

The source of external gradient fields can often be linked to some nearby *dipole* – a research magnet, a steel door, or even a passing vehicle³. A very important example to study then is the field of the physical dipole, or current loop, expressed in spherical coordinates. More complicated magnetic structures can often be modelled from a superposition of such loops or, as mentioned before, using a decomposition into general spherical har-

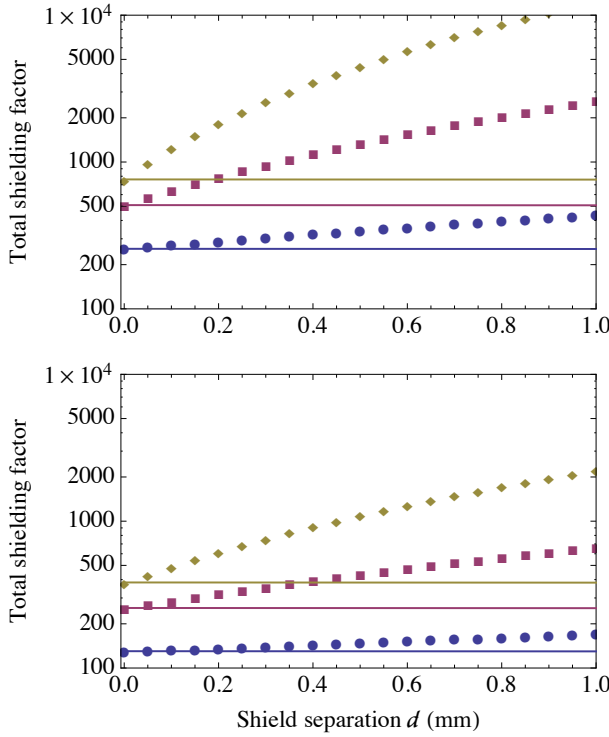


FIG. 4. The total shielding factor of four closely-spaced concentric cylindrical shells of permeability $\mu/\mu_0 = 4 \times 10^4$ (top) and 2×10^4 (bottom) determined from Eq. 21 for an applied field of $n = 1$ (blue circles), 2 (red squares), and 3 (yellow diamonds). The solid lines are the results of Eqs. 41 and 12, and are a very weak inverse function of d .

monics.³⁴

Here we consider a circular loop of radius r_c carrying current I that is co-axial with z -axis and lying in the plane $z = z_c$. The loop can also be viewed as lying on a sphere of radius $a = \sqrt{r_c^2 + z_c^2}$ at the polar angle $\alpha = \tan^{-1} r_c/z_c$. The magnetic field of the loop can be decomposed into zonal harmonics^{26,27} and therefore its interaction with spherical shields is easily determined using the results of Sec. IV.

For example, in the region $r < a$ the magnetic field components of the loop are

$$\begin{pmatrix} B_r \\ B_\theta \end{pmatrix} = \frac{\mu_0 I \sin \alpha}{2a} \sum_{n=1}^{\infty} \left(\frac{r}{a} \right)^{n-1} P_n^1(\cos \alpha) \times \begin{pmatrix} -P_n(\cos \theta) \\ P_n^1(\cos \theta) \end{pmatrix}. \quad (42)$$

All that remains is to multiply each n component of the field by the appropriate shielding factor from Sec. IV C to determine the interior field. Furthermore, the reflected exterior field, dominated by the response of the outermost magnetic shield, may be determined by applying the results of Sec. IV B to each n component. An appropriate sensor and coil system to effectively cancel particularly problematic external dipoles of this sort can then

be devised.

C. Generation of a uniform internal field

A critical requirement of many experiments^{8–11} is the generation of a highly uniform magnetic field in the inner volume of a passive shield system. If the coils used to generate this field are not *self-shielded* in some manner³⁵ they will couple strongly to the shields. This coupling, if taken into account properly, can be used advantageously to improve the field homogeneity over the case where no passive shielding is present. In order to accentuate this point, and to illustrate the power of our formulation, we present two simple, canonical examples – the saddle-shaped coil and the Helmholtz coil.

In the cylindrical case, a saddle-shaped coil can be used to produce a transverse field with a dominant $n = 1$ term near $\rho = 0$. For a very long (infinite) coil, the $n = 2$ term can be eliminated by placing the four axial current paths at $\phi = \pm\frac{\pi}{3}$ and $\pm\frac{2\pi}{3}$.³⁵ An end view of the geometric arrangement of the currents is shown in Fig. 5. Using the results of Ref.³⁵ along with Eq. 26 from above, the components of the internal field of such a coil inside a high- μ cylindrical shield are

$$\begin{pmatrix} B_\rho \\ B_\phi \end{pmatrix} = \frac{2\mu_0 I}{\pi a} \sum_{n=1,5,7,\dots}^{\infty} \sin(n\frac{\pi}{3}) \left(\frac{\rho}{a} \right)^{n-1} \times \left[1 + \left(\frac{a}{R} \right)^{2n} \right] \begin{pmatrix} \cos n\phi \\ -\sin n\phi \end{pmatrix}, \quad (43)$$

where the sum is over odd n not equal to an integer multiple of 3. Provided that the coil is not located directly on the inner surface of the shield (i.e., $a < R$) the resulting field is always more homogeneous than an unshielded coil ($R \rightarrow \infty$), because the term in square braces – the reaction factor – is greatest for $n = 1$ and decreases for all higher order terms.³⁶

As can be seen from the plot in Fig. 5, however, there must exist a value of a/R for which the ratio of the reaction factor for $n = 5$ compared to that for $n = 1$ is a minimum. One can show that this occurs at $a/R = 0.7784$ and that for a coil located at this position the $n = 5$ term is $\sim 33\%$ lower relative to the $n = 1$ term then compared to the unshielded case. This result demonstrates that field homogeneity can be obtained not only by appropriate coil design but also by a judicious choice of a for the location of the coil inside the shield.

Turning to the spherical case, a Helmholtz coil can be used to produce an axial field with a dominant $n = 1$. The coil is constructed from two current loops located at $z = \pm r_c/2$ (as shown in Fig. 5), or equivalently at angles α and $\pi - \alpha$ where $\sin \alpha = 2/\sqrt{5}$ and $\cos \alpha = 1/\sqrt{5}$. Since $\sin(\pi - \alpha) = \sin \alpha$, $\cos(\pi - \alpha) = -\cos \alpha$, and $P_n^1(u)$ is an even (odd) function of u for odd (even) degree n , only the odd n terms of Eq. 42 contribute to net field. Furthermore, since $P_3^1(\pm 1/\sqrt{5})$ is uniquely zero – thereby

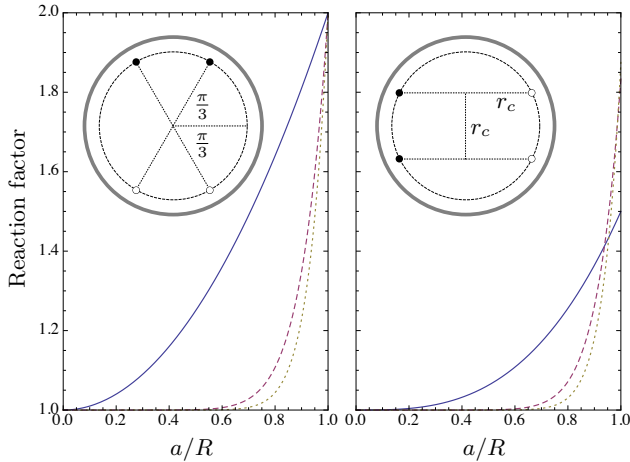


FIG. 5. The reaction factor for $n = 1$ (solid line), 5 (dashed line), and 7 (dotted line) from Eqs. 26 and 39 for the cylindrical (left) and spherical (right) case, respectively. Insets: Schematic of a saddle coil (left) and Helmholtz coil (right) located on the radius a (dashed line) inside a shield (thick gray line) of inner radius R . The dotted lines define the geometry of the coil and give the locations of the current (circles). The closed (opened) symbols indicate current flow out of (into) the page.

eliminating the $n = 3$ term – the field components can be written as

$$\begin{pmatrix} B_r \\ B_\theta \end{pmatrix} = \frac{2\mu_0 I}{\sqrt{5}a} \sum_{n=1,5,7,\dots}^{\infty} \left(\frac{r}{a}\right)^{n-1} P_n^1(1/\sqrt{5}) \times \begin{pmatrix} -P_n(\cos\theta) \\ P_n^1(\cos\theta) \end{pmatrix}. \quad (44)$$

The expansion of Eq. 44 in $r = z$ at $\theta = 0$ gives the following leading order terms – corresponding here to $n = 1$ and 5 – for the field along the central axis:

$$B_z = B_c \left(1 - \frac{144}{125} \left(\frac{z}{r_c} \right)^4 + \dots \right), \quad (45)$$

where $B_c = \mu_0 I / r_c \times (4/5)^{3/2}$ is the well-known central field of a Helmholtz coil.

If the coil is now placed inside a high- μ spherical shield of inner radius $R > a$, the relative strength of these terms will vary according to Eq. 39, and as plotted in Fig. 5. One can show that for $a/R = 0.7817$ the ratio of the reaction factor for $n = 5$ compared to that for $n = 1$ is a minimum and the relative strength of the z^4 term is reduced by $\sim 15\%$ compared to the unshielded coil. For $a/R > 0.9381$, where the reaction factor of the $n = 5$ term becomes greater than that for $n = 1$, the homogeneity near the origin is in fact degraded. This highlights the care that must be taken in designing shield-coupled coils, even in ideal geometrical situations.

VI. CONCLUSION

In this paper, we have provided a comprehensive framework of analytical results that are useful to analyze magnetic shielding systems possessing cylindrical or spherical symmetry. The results are general to any shields possessing this symmetry, placed in any exterior or interior dc current distribution that can be decomposed into multipoles. We have provided here but a few examples demonstrating the utility of the approach, using our formulae to analyze coil systems placed close to magnetic shields.

A key general finding is that higher order multipoles n are always shielded progressively better than the uniform field $n = 1$ case. Furthermore, judicious choices in geometry can make good designs of homogeneous internal coil systems even better when placed internal to a system of magnetic shields. But the work goes beyond these findings in allowing general magnetic shielding and coil system designs to be studied.

In future work, we intend to study the deviations from these results when more realistic geometries are considered, such as finite cylindrical shields with end caps and apertures for experimental access. Such problems do not generally afford analytic solutions, and one naturally must resort to finite element analysis (FEA) codes to conduct such a study. As a result, we envision first benchmarking FEA code to the analytic formulae provided here for an ideal case approximating the eventual desired coil and shield system. Changes are then made in the FEA model to represent more realistic coils and/or shields, and the deviation from the ideal case quantified. We believe that in such a manner our results presented here will be applicable to broad classes of coil and shielding systems, as an important starting point toward achieving design goals.

ACKNOWLEDGMENTS

We gratefully acknowledge the support of the Natural Sciences and Engineering Research Council of Canada.

¹J. Bork, H.D. Hahlbloom, R. Klein, and A. Schnabel, “The 8-layered magnetically shielded room of the PTB: Design and construction,” Proceedings of the 12th International Conference on Biomagnetism (2000).

²D. Cohen, U. Schlapfer, S.P. Ahlfors, M.S. Hmlinen, E. Halgren, “New six-layer magnetically-shielded room for MEG,” Proceedings of the 13th International Conference on Biomagnetism (2002).

³T. Brys, *et al.*, “Magnetic field stabilization for magnetically shielded volumes by external field coils,” *Nucl. Instrum. Meth. A* 554, 527 (2005).

⁴M. D. Swallows, T. H. Loftus, W. C. Griffith, B. R. Heckel, E. N. Fortson, and M. V. Romalis, “Techniques used to search for a permanent electric dipole moment of the ^{199}Hg atom and the implications for CP violation,” *Phys. Rev. A* 87, 012102 (2013).

⁵S. Groeger, J.-L. Schenker, R. Wynands, and A. Weis, *Eur. Phys. J. D* 38, 239 (2006).

⁶D. Budker and M. V. Romalis, *Nat. Phys.* 3, 227 (2007).

⁷T. W. Kornack, S. J. Smullin, S.-K. Lee, and M. V. Romalis "A low-noise ferrite magnetic shield," *Appl. Phys. Lett.* **90**, 223501 (2007);

⁸J.M. Pendlebury *et al.*, *Phys. Rev. A* **70**, 032102 (2004).

⁹S.K. Lamoreaux and R. Golub, *Phys. Rev. A* **71**, 032104 (2005).

¹⁰P. G. Harris and J. M. Pendlebury, *Phys. Rev. A* **73**, 014101 (2006).

¹¹A. L. Barabanov, R. Golub, and S. K. Lamoreaux, *Phys. Rev. A* **74**, 052115 (2006).

¹²A.P. Wills, On the magnetic shielding effect of trilamellar spherical and cylindrical shells, *The Physical Review* **9**, 193-213 (1899).

¹³T.E. Sterne, Multi-lamellar cylindrical magnetic shields, *Review of Scientific Instruments* **6**, 324-326 (1935).

¹⁴W.G. Wadey, Magnetic shielding with multiple cylindrical shells, *Review of Scientific Instruments* **27**, 910-916 (1956).

¹⁵F. Schweizer, Magnetic shielding factors of a system of concentric spherical shells, *Journal of Applied Physics* **33**, 1001-1003 (1962).

¹⁶A.K. Thomas, Magnetic Shielded Enclosure Design in the DC and VLF Region, *IEEE Transactions on Electromagnetic Compatibility* **10**, 142-152 (1968).

¹⁷A. Mager, Magnetic shields, *IEEE Transactions on Magnetics* **6**, 67-75 (1970).

¹⁸S.M. Freake and T.L. Thorp, Shielding of low magnetic fields with multiple cylindrical shields, *Review of Scientific Instruments* **42**, 1411-1413 (1971).

¹⁹D.U. Gubser, S.A. Wolf, and J.E. Cox, Shielding of longitudinal magnetic fields with thin, closely spaced, concentric cylinders of high permeability material, *Review of Scientific Instruments* **50**, 751-756 (1979).

²⁰D. Dubbers, Simple formula for multiple mu-metal shields, *Nuclear Instruments and Methods in Physics Research* **A243**, 511-517 (1986).

²¹T.J. Sumner, J.M. Pendlebury, and K.F. Smith, Conventional magnetic shielding, *J. Phys. D: Appl. Phys.* **20**, 1095-1101 (1987).

²²J.F. Hoburg, Principles of quasistatic magnetic shielding with cylindrical and spherical shields, *IEEE Transactions on Electromagnetic Compatibility* **37**, 574-579 (1995).

²³L. Urankar and R. Oppelt, Design criterions for active shield-
ing of inhomogeneous magnetic fields for biomagnetic applications, *IEEE Transactions on Biomedical Engineering* **43**, 697-707 (1996).

²⁴E.A. Burt and C.R. Ekstrom, Optimal three-layer cylindrical magnetic shield sets for scientific applications, *Review of Scientific Instruments* **73**, 2699-2704 (2002).

²⁵E. Paperno, S. Peliwal, M.V. Romalis, and A. Plotkin, Optimum shell separation for closed axial cylindrical magnetic shields, *Journal of Applied Physics* **97**, 10Q104 (2005).

²⁶W.R. Smythe, *Static and Dynamic Electricity*, 2nd ed. (McGraw-Hill, New York, 1950). See §7.12 and §7.17.

²⁷V.C.A. Ferraro, *Electromagnetic Theory*, (Athalone Press, London, 1967). See §186, §235, and §236.

²⁸D.E. Lobb, Properties of some useful two-dimensional magnetic fields, *Nuclear Instruments and Methods* **64**, 251-267 (1968).

²⁹J.D. Jackson, *Classical Electrodynamics*, 3rd ed. (Wiley, New York, 1999).

³⁰H. Kaden, *Wirbelströme und Schirmung in der Nachrichtentechnik*, 2nd ed. (Springer-Verlag, Berlin, 1959).

³¹A. Nussbaum, *Electromagnetic Theory for Engineers and Scientists*, (Prentice-Hall, Englewood Cliffs, 1965).

³²E. Durand, *Magnétostatique*, (Masson et Cie, Paris, 1968).

³³An example of such code, written in Mathematica, is available from the authors upon request.

³⁴F. Roméo and D.I. Hoult, Magnet field profiling: analysis and correcting coil design, *Magnetic Resonance in Medicine* **1**, 44-65 (1984).

³⁵C.P. Bidinosti, I.S. Kravchuk, and M.E. Hayden, Active Shielding of Cylindrical Saddle-shaped Coils: Application to Wire-wound RF Coils for Low-Field NMR and MRI, *Journal of Magnetic Resonance* **177**, 31-43 (2005).

³⁶It is informative to contrast this with the case of a superconducting or perfectly conducting shield, where free currents induced on the inner surface of the shield act to reduce the field in the region $\rho < a$. In this case, the term in square braces is replaced by $[1 - (a/R)^{2n}]$ (as given in Eq. 31 of Ref.³⁵) and the field becomes less homogeneous in the presence of the shield.